Tubular Multi-Bilayer Polysaccharide Biofilms on Ultra-Thin Cellulose Fibers

Bin Ding, Jian Du, You-Lo Hsieh

Fiber and Polymer Science, University of California, Davis, California 95616

Received 19 July 2010; accepted 5 December 2010
DOI 10.1002/app.33955
Published online 23 March 2011 in Wiley Online Library (wileyonlinelibrary.com).

ABSTRACT: Multiple bilayered polysaccharide biofilms have been assembled by electrostatic layer-by-layer (LBL), alternating deposition of cationic chitosan (CS, M_v = 405 kDa) and anionic dextran sulfate (DXS, M_w = 500 kDa) onto ultra-fine cellulose (CELL) and partially hydrolyzed cellulose acetate fibers with diameters ranging from 350 to 410 nm. While the surfaces of partially hydrolyzed (degrees of substitution of 1.14 or 0.2) and CELL fibers were equally hydrophilic, higher surface charges on the more hydrolyzed fibers afford thicker bilayers. The elestrostatic interactions between CS and DXS were enhanced by the presence of NaCl in the dipping and rinsing solutions to allow uniform deposition of sequential polysaccharide bilayers. At 0.25*M* NaCl, each CS/DXS bilayer averaged 6.4 to 9.0 nm thick with the total thickness of the five bilayer $(CS/DXS)_5$ varied from 64 to 77 nm. The CS/DXS bilayers exhibited much reduced BET surface area and pore volume indicating that these polysaccharides were much more densely packed on the fully hydrolyzed CELL fibers. The findings proofed the concept that long chain polysaccharide electrolytes can be self-assembled as nanometer scale tubular bilayers on ultra-fine cellulose fibers to afford wholly polysaccharidic fibrous architecture. The electrolytic nature, chemical reactivity, and structural versatility of these ultra-high specific surface polysaccharides are advantageous and can be further tuned to serve biological functions and for biomedical applications. © 2011 Wiley Periodicals, Inc. J Appl Polym Sci 121: 2526–2534, 2011

Key words: layer-by-layer (LBL); deposition; polysaccharide biofilm; chitosan; dextran sulfate; cellulose fibers; electrospinning; tubular bilayer

INTRODUCTION

For many decades, fabrication of nanostructured films on solid surfaces has been dominated by the Langmuir-Blodgett (LB) technique in which a self-assembled monolayer formed on a water surface is transferred onto a solid surface.[1] The LB deposition is based on the ability of polar molecules with hydrophilic heads and hydrophobic tails to organize into well defined monolayers at the water–air interface, therefore, is limited to molecules capable of such behavior. These deposited molecules may not be firmly anchored on the surfaces and can rearrange themselves following or sometimes during deposition.

The electrostatic layer-by-layer (LBL) self-assembly involves the step-wise, alternating adsorption of oppositely charged electrolytes on solid surfaces to form well-defined composition and structure at nanometer scale precision.[2–4] The electrostatic force principle enables the deposition of a much wider range of charged species, including chemically and structurally diverse macromolecules,[5] organic and inorganic compounds[6] as well as DNA[7] and enzymes.[8,9] The simplicity of LBL process also lends itself to deposition on a great variety of solid substrates with different chemistries, shapes, and sizes, including metal nanorods,[10] metal nanoparticles,[11] short inorganic fibers,[12] and polymer microspheres.[13]

In the areas of polyelectrolyte multi-layer (PEM) films, work to date has been dominated by synthetic polyeletrolytes. Polysaccharides, the major constituents to plant and animal cells and functions, have received much less attention as sources of functional materials. Few have attempted to assemble LBL of polysaccharides.[14] Polysaccharides (chitosan, heparin, and hyaluronan) have been coated on gold and polystyrene surfaces.[15] Polysaccharide derivatives (carboxymethyl cellulose, carboxymethylpullulans) have been assembled with synthetic polyelectrolytes (polyethylenimine, polydiallyldimethylammonium)[16] and proteins.[17] LBL of polypeptides (poly-L-lysine, poly-L-glutamic acid) and polysaccharides (chitosan/dextran sulfate) have been assembled onto soft and porous (*N*-isopropylacrylamide-*co*-methacrylic acid) microgels.[18] We have encapsulated lipase enzyme in LBL fashion with reactive dye ligand to ultra-fine cellulose fibrous membrane.[9] Assembling oppositely charged polysaccharides in alternating

Correspondence to: Y.-L. Hsieh (ylhsieh@ucdavis.edu).
Contract grant sponsor: National Textile Center; contract grant number: M04-CD06.

fashion onto polysaccharide solids is not well understood.

This study was to investigate LBL deposition of oppositely charged ionic polysaccharides on ultra-thin cellulose fibers to form multiple bilayers of biofilms. The goals of this work were to understand the surface effects of cellulose fibers on LBL deposition of polysaccharides, to establish multiple bilayers on ultra-thin fibers and to characterize the structure of multiple LBL polysaccharide bilayer deposited cellulose fibers. The cellulose fiber templates employed were generated by electrospinning of cellulose acetate (CA) followed by alkaline hydrolysis to cellulose (CELL).[19] This approach has shown to be robust and highly versatile to fabricate cellulose fibrous membranes with targeted fiber diameters ranging from 50 nm to several hundred nm and wide ranging fiber packing and interfiber pore morphologies by simple choice of solvent systems, electrospining and collection methods. In this study, membranes with fibers of less than 500 nm diameters were employed for easy handling in multiple solution dipping and rising processes.

Two significant polysaccharides, i.e., chitosan (CS) and dextran sulfate (DXS), were selected for their electrolytic properties as well as their biological significance and chemical reactivity. Chitosan is polycationic. Because of its unique antimicrobial activity and compatibility to a variety of mammalian cell types, chitosan has received a great deal of attention as a material of choice for delivery of drugs, proteins and peptides, cell culturing, and biocidic films.[20] The ability of chitosan to bind azo compounds has been demonstrated for light storage.[21] Dextran sulfate is polyanionic and has long been applied as antiadhesive and anticoagulant agent[22] and, like heparin, has proved to be potent and selective inhibitors of human immunodeficiency virus activity *in vitro*.[23] In fact, buildup mechanism of chitosan and heparin multiple bilayers on silicon wafers and titanium alloys has been studied by electrochemical and imaging techniques.[24]

Integrating polysaccharides in any structure, in particular as nanoscale biofilms and on ultra-high specific surface fibrous and porous materials, provides new biologically derived advanced materials with their multiple inherent biological properties. The reactivities of both polysaccharides, i.e., chitosan's amine and hydroxyl groups and dextran's sulfate and hydroxl groups, offer ample opportunities to add yet further functional properties. Furthermore, these nano-structured polysaccharidic assemblies have potential to incorporate many diverse materials such as charged particles, inorganic and organic compounds, proteins and enzymes for miniaturized devices and functional bio-based materials.

MATERIALS AND METHODS

Materials

The polymer used included cellulose acetate (CA) with a degree of substitution (DS) of 2.45 (M_n = 30 kDa, Aldrich), chitosan (CS, M_v = 405 kDa, Aldrich), and dextran sulfate (DXS, M_w = 500 kDa, EM Science). CS with M_v of 190 kDa was obtained by alkaline hydrolysis (40 wt % aqueous NaOH) of the 405 kDa CS at ambient temperature for 4 days. Acetone (Fisher Scientific), *N*,*N*-dimethylacetamide (DMAc) (EM Science), ethanol (EM Science), acetic acid (99.7%, EM Science), sodium hydroxide (EM Science), hydrogen chloride (EM Science), sodium bicarbonate (Fisher Scientific), sodium chloride (Fisher Scientific), poly(diallyldimethylammonium chloride) (PDADMAC, M_w = 170 kDa; 20 wt %, Aldrich), poly(vinyl sulfate, potassium salt) (PVSK) (M_w = 170 kDa, Aldrich), and toluidine blue O (Sigma-Aldrich) were used without further purification. Purified water from the Milli-Q^{TM} Water System with a resistance of 10 MΩ was used for LBL deposition.

Fabrication of cellulose fibrous templates

Fibrous template was generated by electrospinning of a 15 wt % CA solution prepared in a 2 : 1 w/w acetone/DMAc mixture. The CA solution was placed in a syringe that was connected to the positive electrode of a high voltage power supply (Gamma High Voltage Supply, ES 30-0.1 P). Electrospinning of the CA solution was conducted at a 1 mL h^{-1} feeding rate using a syringe pump (Model 780200, KD Scientific) and a 15 kV applied voltage. The fibrous template was collected on the surface of a grounded aluminum foil at a 22-cm tip-to-collector distance.

The CA fibrous templates was hydrolyzed in 0.05*M* NaOH aqueous or ethanol solutions at ambient temperature following previously report procedures.[25] Briefly, CA with a DS of 0.2 was obtained by hydrolysis in NaOH/ethanol (0.05*M*) for 30 min. Meanwhile, CA with a DS of 1.14 was prepared by aqueous hydrolysis (0.05*M*) at ambient temperature for 140 min. Complete hydrolysis to generate CELL fibrous templates was conducted in 0.05*M* NaOH aqueous solution at ambient temperature for 4 days. The CA fibrous templates with DS of 2.45, 1.14, and 0.2 were denoted as CA2.45, CA1.14, and CA0.2, respectively.

Formation of LBL structured polysaccharides on cellulose template fibers

Bilayers of oppositely charged CS and DXS were formed on the surfaces of negatively charged cellulose template fibers by alternating layer-by-layer

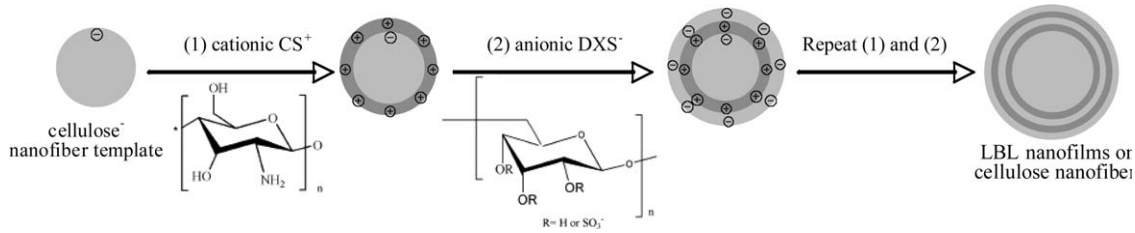

Figure 1 Schematic diagram illustrating LBL deposition of chitosan (CS) and dextran sulfate (DXS) as bilayer self-assembled biofilms on cellulose (CELL) nanofibers.

(LBL) deposition via electrostatic forces as illustrated (Fig. 1). The dipping aqueous solutions of CS and DXS were prepared at the same fixed 1 mg mL^{-1} concentration at ambient temperature with vigorous stirring. The pH values of the CS and DXS solutions were adjusted to 5 and 6, respectively, with either HCl or NaOH solutions (1 mol L^{-1}). The pH value of rinsing solutions was fixed at 6. The ionic strengths of the CS, DXS, and rinsing solutions were regulated by adding NaCl at 0.25 and 0.5 mol L^{-1} concentrations. The deposition of LBL films were performed by first immersing the cellulose fibrous templates into CS solution for 20 min followed by three 2-min water rinses, fresh each time. The templates then were immersed into the DXS solution for 20 min followed by identical rinsing steps. The adsorption and rinsing steps were repeated until the desired number of bilayer was obtained. The LBL films-coated fibrous templates were washed with water and dried at 80°C under vacuum for 10 h to remove the solvent. The LBL film-coated samples were labeled as a-$(CS/DXS)_b$-c, where a denoted the type of template fibers, b the number of bilayer, and c the NaCl concentration.

Characterization

The negative surface charge of the template fibers was measured using polycationic electrolyte PDADMAC (M_w = 170 kDa) which was deemed more appropriate for correlating to the adsorption of the two polysaccharide electrolytes of CS (M_v = 190 kDa) and DXS (M_v = 405 kDa). Surface charges were measured by titration of the residual polycations in the solution. All fibrous samples were first immersed into 0.1M $NaHCO_3$ (adjusted to pH 9 with 0.1M NaOH) for 1 h. The fibrous samples were washed with deionized water and dried at 80°C under vacuum for 6 h. The dry fibers (0.15 g) were then immersed in 40 mL aqueous PDADMAC (1 g L^{-1}) and NaCl (0.05M) mixture at pH 7 for 1 h. The suspensions were filtered and the fibers were washed with additional aqueous 0.05M NaCl solution to remove the unadsorbed PDADMAC and reach a total filtrate of 60 mL. Each 10 mL filtrate with added toluidine blue O was titrated using aqueous PVSK solution (1 g L^{-1}). Blank samples, which contained only the cationic polymers PDADMAC, were titrated the same to correct the titration. The surface charge (Q_S) of the fibers was calculated as:

$$Qs = \frac{(V_0 - V_{\text{tit}})C_{\text{polymer}}}{m_{\text{dry}}} \cdot \frac{V_{\text{tot}}}{V_{\text{sample}}}$$

where V_0 and V_{tit} were the volume (mL) of titrant used for blank and fiber sample, respectively; C_{polymer} and V_{tot} was the concentration (mol L^{-1}) and total volume of the titrant, respectively; V_{sample} was the volume of filtrate suspension used for titration; and m_{dry} was the dry sample mass. The average of at least three measurements was reported for each sample.

The morphology of the fibrous samples was examined by a scanning electron microscope (SEM, Philips, FEI XL30s FEG). The average fiber diameter of each sample was determined by a total of 100 measurements from SEM images of various sample areas using an image analyzer (Adobe Photoshop 7.0). Fourier transform infrared (FT-IR) spectra of fibrous samples were collected from 4000 to 400 cm^{-1} at 128 scans with a 4 cm^{-1} resolution using a Nicolet Magna-IR 560 spectrometer. The Brunauer-Emmett-Teller (BET) surface area, pore volume, and pore width of the fibrous samples were characterized by nitrogen gas adsorption (Micromeritics, ASAP 2020 analyzer). Water contact angle of fibrous samples was determined by a surface tensiometer (KRUSS, K14) according to a previous reported procedure.[26]

RESULTS AND DISCUSSION

Cellulose fibrous template

Ultra-fine cellulose fibers was prepared by electrospinning cellulose acetate (CA2.45) into fibrous templates and then hydrolyzed to varying degrees of substitution (DS) of 1.14, 0.2, and 0. The as-spun CA2.45 fibrous template consisted loosely packed cylindrical fibers with an average diameter of 351 nm [Fig. 2(a), Table I]. Alkaline hydrolysis generally caused the fibers to pack more closely, particularly

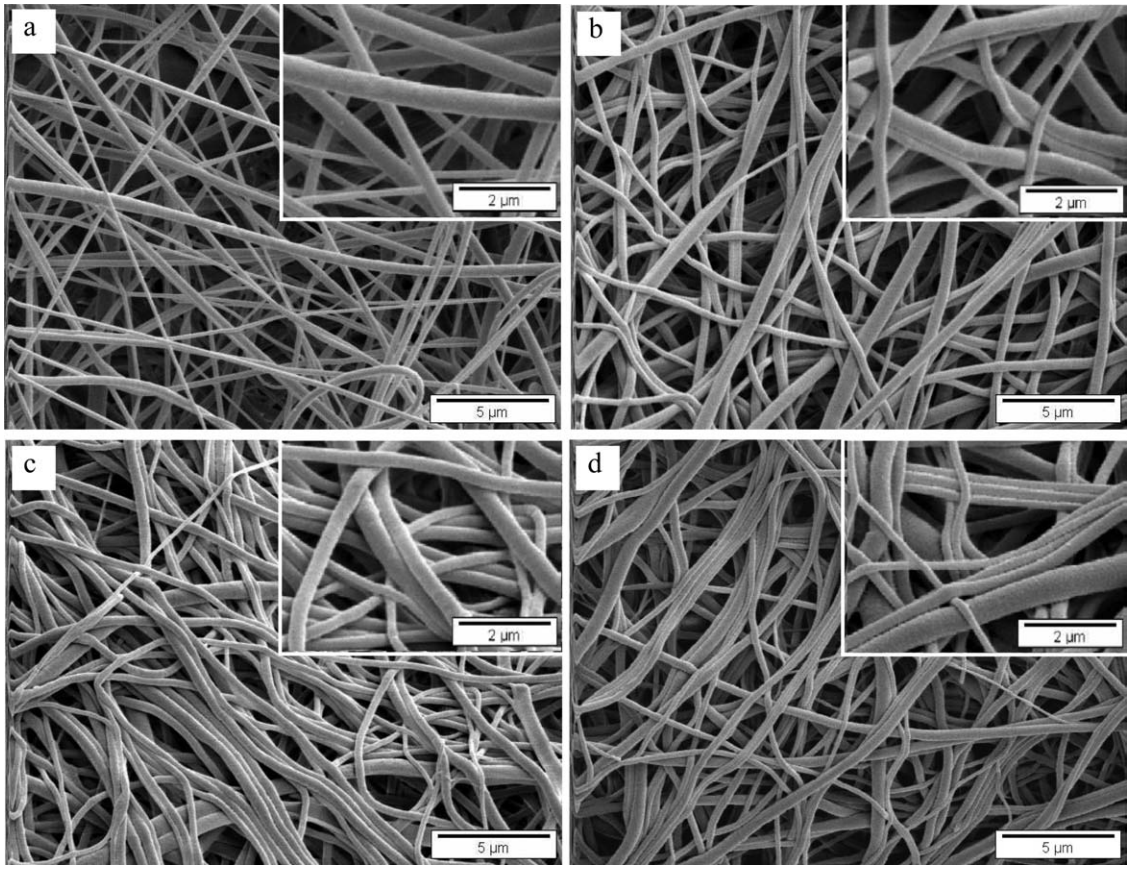

Figure 2 SEM images of template fibers: (a) CA2.45, (b) CA1.14, (c) CA0.2, and (d) CELL.

in the thickness direction of the membrane, and merge with adjacent fibers along the lengths and at crossover junctions [Fig. 2(b,c)]. This is expected from the increasing capacity of the fibers to hydrogen bond with each other with increasing hydrolysis or conversion of the acetyl to hydroxyl groups. Although coefficient of variance of the fiber dimensions varied from 29 to 41% among the four template fibers, the averaged fiber diameters showed an increasing trend from 351 nm to 377 and 413 nm at DS of 1.14 and 0.2, respectively, (Table I). The fully hydrolyzed CELL fibers showed no additional change in their overall appearance [Fig. 2(d)].

The FTIR of the as-spun CA2.45 [Fig. 3(a)] showed a strong characteristic acetyl carbonyl peak around 1740 cm^{-1} ($\upsilon_{C=O}$) and an ether peak around 1640 cm^{-1} (υ_{C-O-C}). The intensities of the acetyl carbonyl at 1740 cm^{-1} decreased with increasing levels of hydrolysis, or decreasing DS, of hydrolyzed template fibers [Fig. 3(b–d)]. This is consistent with the expected nucleophilic substitution of the acetyl groups with hydroxyl groups. The acetyl carbonyl peak became indistinguishable for CELL, confirming complete conversion of acetyl to hydroxyl and full hydrolysis [Fig. 3(d)].

The surface wetting behavior of a solid governs the spreading and contact of the surface with a liquid and is critical to the LBL dipping and rinsing processes. Water wetting contact angles of the template fibrous templates reduced from 87.1° to 30.6° with decreasing DS from 2.45 to 0.2 (Table I). The conversion of acetyl to hydroxyl led to significantly

TABLE I
The Characteristics of Template Fibers

Template	Surface charge (mmol/g)	Average fiber diameter (nm)	BET surface area (m^2/g)	Pore volume (cm^3/g)	Pore diameter (nm)	Water contact angle (°)
CA2.45	1.32±0.07	351±148	3.80	0.008	9.0	87.1±1.9
CA1.14	1.56±0.03	377±109	3.84	0.012	12.0	29.3±1.1
CA0.2	2.15±0.03	413±159	3.97	0.014	14.3	30.6±6.2
CELL	2.05±0.06	410±130	5.01	0.017	13.6	32.8±1.1

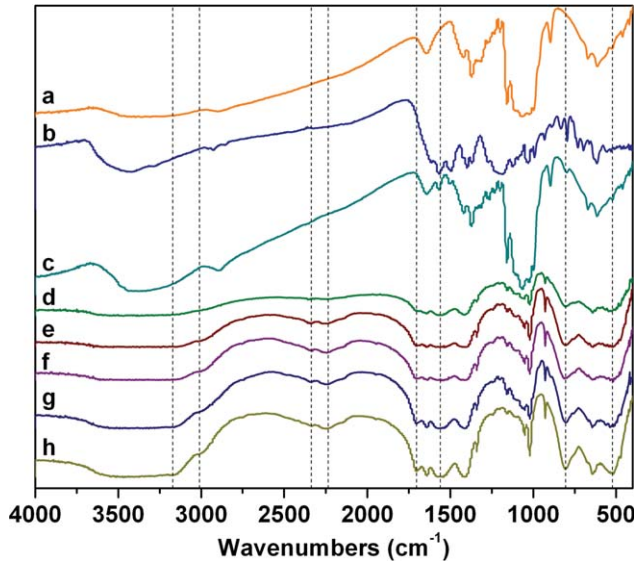

Figure 3 FTIR spectra of template fibers: (a) CA2.45, (b) CA1.14, (c) CA0.2, and (d) CELL. [Color figure can be viewed in the online issue, which is available at wileyonlinelibrary.com.]

improved water wettability as expected. In fact, the surface of the fibrous membrane containing over a third of the acetyl content (1.14 DS) was as wettable by water as that of the CELL fibers. The fact that both partially hydrolyzed fibers (CA1.14 and CA0.2) have the same water wetting contact angles as the fully hydrolyzed CELL fibers indicates that the surfaces of the partially hydrolyzed fibers are fully hydrolyzed as the CELL fibers while their bulks are not. The similar physical contacts and closely packed structure of the partially (1.14 and 0.2 DS) and fully hydrolyzed CELL fibers shown in Figure 2(b–d) are consistent with their fully hydrolyzed surfaces whose abundant hydroxyl groups help to bring fibers together by hydrogen bonds.

The surface charge property of the template fibers is critical to the deposition of the first monolayer of electrolytes. The negative surface charges of the template fibers were measured using polycationic electrolyte PDADMAC (M_w = 170 kDa). The CA2.45 fibrous templates had an average surface charge of 1.32 mmol g^{-1} (Table I). With increasing hydrolysis or decreasing DS of 1.14 and 0.2, the surface charge increased to 1.56 and 2.15 mmol g^{-1}, respectively. The surface charge of CELL was 2.05 mmol g^{-1}, slightly lower than that of CA0.2. This observation shows that surface charges of these cellulose template fibers increase with increasing hydrolysis and the CA0.2 fiber surfaces are similarly charged as the

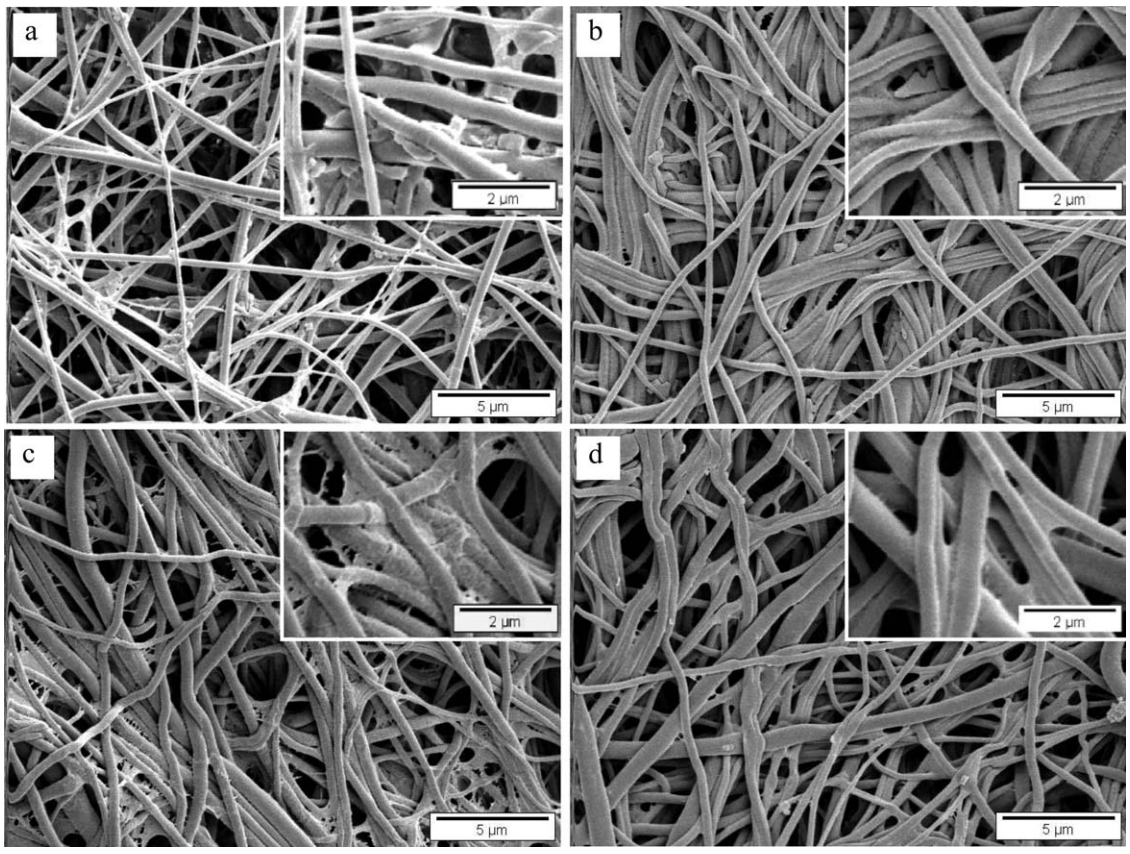

Figure 4 SEM images of $(CS/DXS)_5$ films deposited (0.25*M* NaCl in dipping and rinsing solutions) on various template fibers: (a) CA2.45, (b) CA1.14, (c) CA0.2, and (d) CELL.

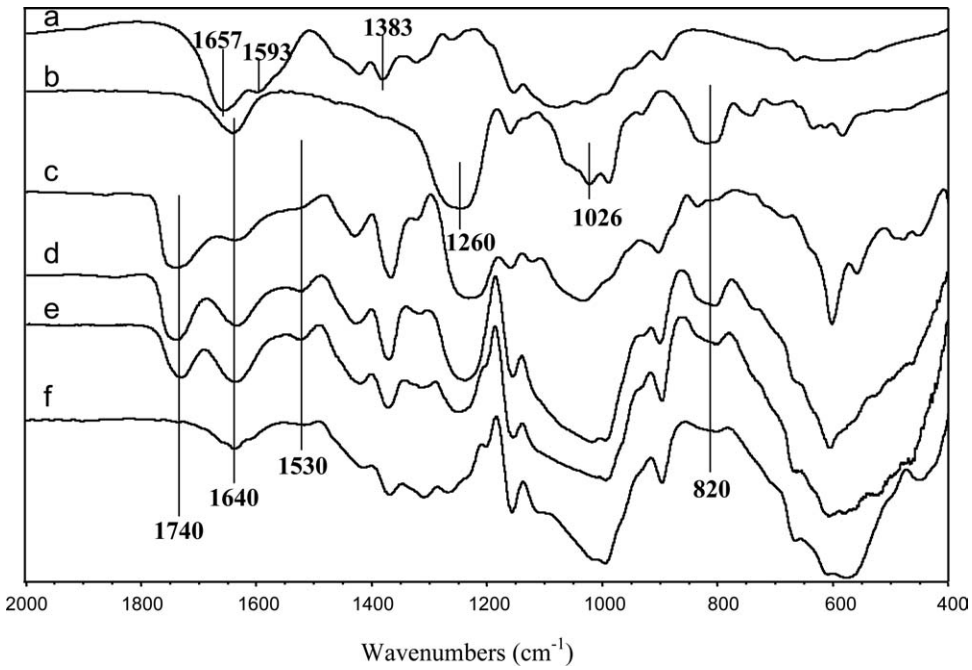

Figure 5 FTIR spectra of (a) CS, (b) DXS, and (c–f) $(CS/DXS)_5$ films deposited (0.25*M* NaCl in dipping and rinsing solutions) on various template fibers: (c) CA2.45, (d) CA1.14, (e) CA0.2, and (f) CELL.

CELL fibers. While the wetting contact angle did not differentiate among the three hydrolyzed template fibers, the surface charges of those with DS at 1.14 and 0.2 were clearly higher, suggesting the surface charge behavior to be more distinguishable to surface hydrolysis than wetting.

The total surface area determined by BET showed a slight increase (4.5%) from 3.8 to 3.97 m^2 g^{-1} with hydrolysis or decreasing DS from 2.45 to 0.2 (Table I). The fully hydrolyzed CELL template showed a significantly higher BET surface area of 5.01 m^2 g^{-1}, a 26% increase from CA0.2. With increasing levels of hydrolysis or decreasing DS from 2.45 to 0.2, both the total pore volumes and mean pore diameters increased, consistent with new internal spaces created by the replacement of the larger acetyl with the substantially smaller hydroxyl groups. From the nearly hydrolyzed (0.2 DS) to the fully hydrolyzed CELL samples, the significant increases in total surface area (by 26%) and pore volume (by 21%) without changes in their mean pore sizes suggest substantially increase in the number of pores. The BET surface area includes both internal and external surfaces of the fibers. While enlargement in fiber sizes reduces external fiber surfaces, increasing number and volume of internal pores increase internal surfaces. The significant higher surface area and pore volume values associated with the final hydrolysis from DS 0.2 to CELL indicate the creation of numerous smaller pores and the increased internal surfaces exceed the reduced external surfaces.

LBL biofilm formation

Five bilayers of CS and DXS or $(CS/DXS)_5$ were deposited at a 0.25*M* NaCl concentration on the template fibers. The LBL deposition of $(CS/DXS)_5$ on CA2.45 fibrous templates resulted in irregular surfaces with large aggregates [Fig. 4(a)] whereas that on CA1.14, CA0.2, and CELL template fibers produced even surfaces [Fig. 4(b–d)]. The uneven surface deposition on template CA2.45 fibers was thought to be due to their hydrophobicity and low surface charge. The smooth appearance of the $(CS/DXS)_5$ LBL deposition on the hydrolyzed fibers indicates uniformly coated surfaces, often connecting the adjacent fibers associated by enhanced hydrogen bonded template fibers. Therefore, all hydrolyzed fibers, irrespectively of their DS, appear to be suitable for electrostatic LBL deposition of CS/DXS bilayers.

The five bilayer $(CS/DXS)_5$ deposited with 0.25*M* NaCl increased the average diameters of the CA1.14, CA0.2, and CELL fibers by 64–77 nm, irrespective of the DS of the template fibers (Table II). The average thickness of the $(CS/DXS)_5$ bilayer LBL films on CA1.14, CA0.2, and CELL was 32, 38.5, and 33 nm, respectively. Furthermore, the average thickness of each CS/DXS bilayer was in the 6–8 nm range.

Figure 5 shows the FTIR spectra of CS and DXS as well as the $(CS/DXS)_5$ bilayer coated template fibers. CS exhibited the characteristic amide peaks at 1657 cm^{-1} (Amide I), 1593 cm^{-1} (Amide II), and 1383 cm^{-1} (Amide III) [Fig. 5(a)], consistent with our prior observation on CS.[25] DXS exhibited the typical

TABLE II
Characteristics of LBL Biofilms Coated Celluclose Fibers

Template LBL-NaCl	Average fiber diameter (nm)	Average film thickness (nm)	Average bilayer thickness (nm)	BET surface area (m^2/g)	Pore volume (cm^3/g)	Pore diameter (nm)	Water contact angle (°)
CA2.45-$(CS/DXS)_5$-0.25	362±108	—	—	3.06	0.007	9.2	73.9±3.7
CA1.14-$(CS/DXS)_5$-0.25	441±92	32	64	1.89	0.005	9.8	47.9±2.8
CA0.2-$(CS/DXS)_5$-0.25	490±152	39	7.8	1.98	0.006	12.0	47.9±6.9
CELL-$(CS/DXS)_5$-0	437±128	—	—	4.63	0.015	12.6	36.2±4.8
CELL-$(CS/DXS)_5$-0.25	476±132	33	6.6	2.23	0.005	8.2	44.3±8.8
CELL-$(CS/DXS)_5$-0.5	499±149	45	9.0	1.70	0.006	13.1	46.4±9.0
CELL-$(CS/DXS)_{10}$-0.25	—	—	—	1.57	0.003	8.1	48.4±6.4

C—O—C vibration peak at 1640 cm^{-1} as well as the sulfyl peaks near 1026 cm^{-1} (symmetric SOO^- stretching vibration), 1260 cm^{-1} (asymmetric SOO^- stretching vibration), and 820 cm^{-1} (*S*—O—S vibrations) [Fig. 5(b)], same as reported before.[27] Following the $(CS/DXS)_5$ bilayer LBL deposition on CA2.45 [Fig. 5(c)], the coated fibers showed a higher relative ether-to-carbonyl intensity ratio than that of the original CA2.45 template fibers [Fig. 3(a)] owing to the enhanced 1640 cm^{-1} peak from the overlapping C—O—C in both CA in the template fibers and the DXS deposited. The appearance of a new peak at 820 cm^{-1} was indicative of the *S*—O—S vibrations or the presence of DXS in the $(CS/DXS)_5$ coated CA2.45. Additionally, a new peak around 1530 cm^{-1} indicated the possible presence of intramolecular hydrogen bonding between the deposited CS and DXS polysaccharides. The $(CS/DXS)_5$ assemblies on CA1.14 [Fig. 5(d)] and CA0.2 [Fig. 5(e)] also showed new 1530 and 820 cm^{-1} peaks and an increased ether-to-carbonyl intensity ratio from their respective template fibers [Fig. 4(b,c)]. Moreover, the characteristic peaks of the $(CS/DXS)_5$ bilayers deposited on CA1.14 and CA0.2 [Fig. 5(b,c)] were much stronger than those on CA2.45 [Fig. 5(a)], indicating higher quantities on the more hydrolyzed template fibers. Finally, the 1530 and 820 cm^{-1} peaks were observed on CELL fibers with five $(CS/DXS)_5$ bilayer LBL films [Fig. 5(f)]. This is the clear evidence of the demonstrated success that these two high molecular weight polysaccharides, i.e., CS and DXS, have assembled as LBL structured films on natural CELL fibers, forming entirely polysaccharide tubular nanocomposite fibers.

The water contact angles of $(CS/DXS)_5$ films deposited (at 0.25*M* NaCl) on CA2.45, CA1.14, CA0.2, and CELL template fibers (Table II) were 73.9°, 47.9°, 47.9°, and 44.3°, respectively. The water wetting contact angle of the coated CA2.45 (73.9°) was much closer to the original CA2.45 fibers (87.1°), consistent with the less coated fiber surfaces as evident by SEM and FTIR. The similar water contact angles (around 45°) of the $(CS/DXS)_5$-coated hydrolyzed template fibers indicated that these five-bilayer coatings are uniform and the wettability of coated template fibers was governed by the same outmost layer, i.e., DXS.

The BET surface areas of the $(CS/DXS)_5$ coated (0.5*M* NaCl) fibers decreased with the hydrolysis levels of the template fibers. Deposition of $(CS/DXS)_5$ on CA2.45, CA1.14, CA0.2, and CELL decreased the BET surface area to 19.5, 50.8, 50.1, and 55.5%, respectively, (Table II). The $(CS/DXS)_5$ deposition also reduced the total pore volume of CA2.45, CA1.14, CA0.2, and CELL by 12.5, 58.3, 57.1, and 70.6%, respectively. The much reduced surface and pore volume of the $(CS/DXS)_5$ coated CELL nanofibers indicated a much denser packing of CS and/or DXS on the fully hydrolyzed template fibers. Although the thickness of the $(CS/DXS)_5$ deposition were similar among the template fibers, the polysaccharides in the bilayers were more densely packed on more hydrolyzed template fibers. Again, the much less and uneven LBL deposition on CA2.45 led to the least changes in the total surface area and pore volume in comparison to all other hydrolyzed template fibers.

NaCl and CS/DS LBL bilayers

The effect of solution ion strength on the deposition of the LBL films was studied on the CELL template fibers. The five bilayer deposition conducted without NaCl did not produce observable changes to the fiber morphology and dimension of CELL [Fig. 6(a)]. FTIR spectra of this LBL deposition also showed no evidence of CS or DXS [Fig. 7(a)] when compared to the CELL template fibers [Fig. 3(d)]. However, the $(CS/DXS)_5$ deposition on CELL without NaCl slightly lowered the BET surface area and total pore volume by 7.6 and 11.8%, respectively. These data indicated that the CS and DXS were assembled on the CELL fibers, but the quantity of LBL films was too low to be detected by FTIR. Therefore, the $(CS/DXS)_5$ films deposited without NaCl were speculated to be very thin. The water contact angle (36.2°) of the LBL coated without NaCl was close to that

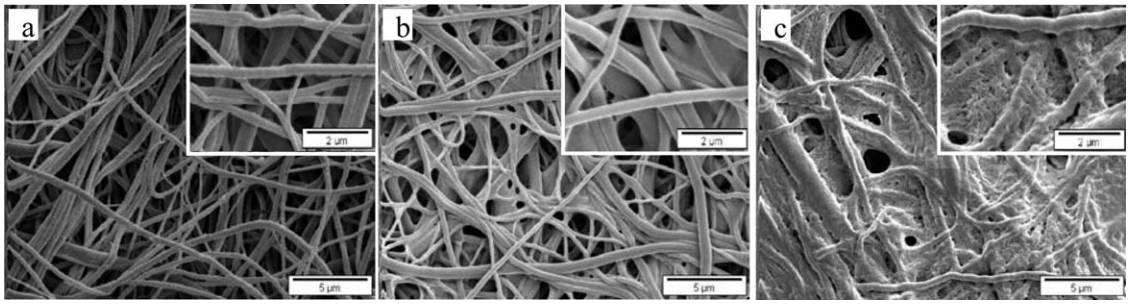

Figure 6 SEM images of CS/DXS LBL films deposited on CELL: (a) $(CS/DXS)_5$ without NaCl, (b) $(CS/DXS)_5$ with 0.5*M* NaCl, and (c) $(CS/DXS)_{10}$ with 0.25*M* NaCl.

(32.8°) of the pure CELL template fibers, confirming little deposition.

The $(CS/DXS)_5$ deposition on CELL increased with the addition of NaCl. At 0.5*M* NaCl, a five-bilayer LBL process produced obvious deposition on fiber surfaces as well as in between adjacent fibers [Fig. 6(b)]. The presence of NaCl was deemed essential to LBL deposition of CS/DXS. The extent of $(CS/DXS)_5$ deposition was also positively associated with the NaCl concentration as it was raised from 0.25 to 0.5*M*. At 0.5*M* NaCl, the fibers were thickened by 45 and 9 nm in the average film and bilayer thickness, respectively. The 1530 and 820 cm^{-1} peak intensities of fibers processed at 0.5*M* NaCl were also stronger [Fig. 7(b)] than those at 0.25*M* NaCl [Fig. 5(f)]. Both fiber dimension and FTIR confirmed $(CS/DXS)_5$ bilayer deposition to be positively influenced by increasing NaCl concentration. The enhanced the quantity and thickness of the $(CS/DXS)_5$ bilayer deposition seems to be consistent with the expectation. However, the five-bilayer LBL deposition at the higher 0.5*M* NaCl concentration also showed further decreases in the BET surface area by 66.1%. The presence of NaCl in the dipping and rinsing solutions decreases the repulsion force among the CS and DXS polyelectrolyte molecules leading to more densely packed layers.

Doubling the CS/DXS bilayers to 10 was evident by the higher deposition as shown [Fig. 6(c)], the increased 1630 and 820 cm^{-1} peak intensities in the FTIR [Fig. 7(c)] and further reduced BET surface area (68.7%). Neither NaCl nor the quantity of the CS/DXS bilayers appears to affect the water wetting behavior of the LBL deposited surfaces. Both are expected as the wetting behavior is determined by the same DXS outermost layer of these surfaces. Similar to early observations, the surface areas reduced with more deposition, either with the higher NaCl concentration or the number of bilayers. However, the effects of NaCl concentration or number of bilayers on pore characteristics are not as clear and require further investigation.

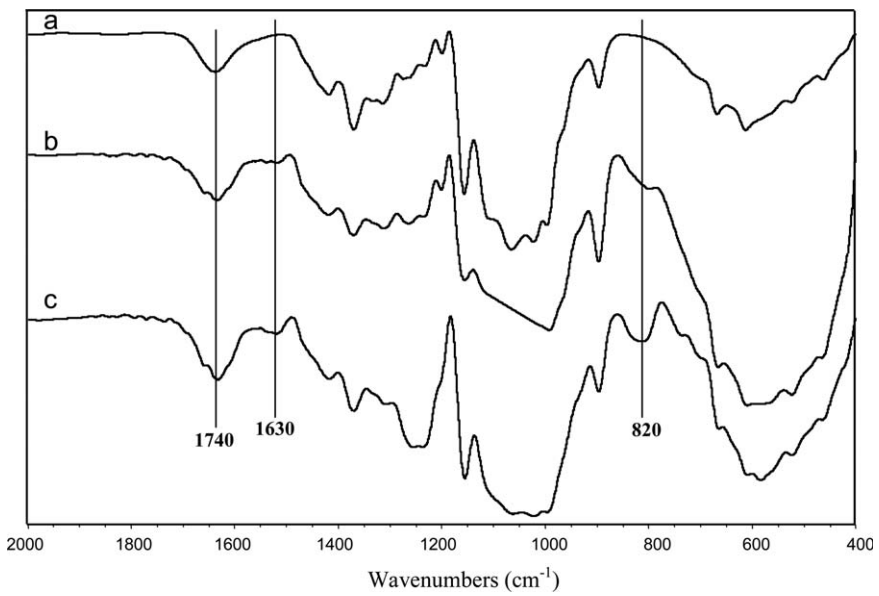

Figure 7 FTIR spectra of CS/DXS LBL films deposited on CELL: (a) $(CS/DXS)_5$ without NaCl, (b) $(CS/DXS)_5$ with 0.5*M* NaCl, and (c) $(CS/DXS)_{10}$ with 0.25*M* NaCl.

CONCLUSIONS

This study demonstrates the feasibility to assemble long chain polysaccharides, i.e., cationic chitosan (CS, M_v = 405 kDa) and anionic dextran sulfate (DXS, M_n = 500 kDa), via the electrostatic LBL technique into nano-scale tubular biofilms on ultra-fine cellulose fibrous templates. Four cellulose fiber templates were prepared by electrospinning cellulose acetate (CA, DS = 2.45), followed by alkaline hydrolysis to varying DS of 1.14, 0.2, and to cellulose (CELL). The nucleophilic substitution of the acetyl group with hydroxyl groups led to significantly improved hydrophilicity of the fiber surfaces and increased pore sizes and pore volume in the fibers. Although all hydrolyzed fibers had essentially the same water wetting contact angles around 30°, the surface charges increased from 1.32 to 1.56 and 2.15 mmol g^{-1} with decreasing DS from 2.45 to 1.14 and 0.2, respectively. Surface hydrophilicity was found critical for uniform LBL deposition whereas higher surface charges increased the thickness of LBL deposition among the three hydrolyzed cellulose fiber templates. The presence of NaCl in the dipping and rising solutions decreased the repulsion among the polyelectrolyte molecules to enhance the quantities and thickness of the CS/DXS LBL bilayers. The total thickness of the five bilayer $(CS/DXS)_5$ tubular biofilms varied from 64 to 77 nm, with averaging CS/DXS bilayer thickness between 6.4 and 9.0 nm. The FTIR gave clear evidence of both CS and DXS and their characteristic peaks intensified with increasing numbers of CS/DXS bilayers on the fibers. The much reduced BET surface area and pore volume of the $(CS/DXS)_5$-coated CELL nanofibers indicated the polysaccharides in the bilayers to be more densely packed on more hydrolyzed template fibers.

The building of multiple nano-scale CS/DXS bilayers on ultra-fine cellulose fibers has demonstrated the prospect of assembling long chain ionic polysaccharides via LBL process on ultra-fine cellulose fibers for new advanced functional materials. The wide-ranging structures of the cellulose fibrous templates, the ability to control the numbers and packing density of nano-scale CS-DXS bilayers and the reactivity of the polysaccharides illustrate the potential to a wide ranging polysaccharidic material scaffold for incorporation, delivery and administration of multiple components of biological significant molecules, such as drugs, peptides, proteins, and gene materials, as well as inorganic and organic materials.

References

1. Blodgett, K. J Am Chem Soc 1934, 56, 495.
2. Bibo, A.; Knobler, C.; Peterson, I. J Phys Chem 1991, 95, 5591.
3. Decher, G.; Hong, J. Macromol Chem Macromol Symp 1991, 46, 321.
4. Decher, G. Science 1997, 277, 1232.
5. Ferreira, M.; Rubner, M. Macromolecules 1995, 28, 7107.
6. Mao, G.; Tsao, Y.; Tirrell, M.; Davis, H.; Hessel, V.; Ringsdorf, H. Langmuir 1993, 9, 3461.
7. Forzani, E.; Solis, V.; Calvo, E. Anal Chem 2000, 72, 5300.
8. Xing, Q.; Eadula, S. R.; Yuri, M.; Lvov, Y. M. Biomacromolecules 2007, 8, 1987.
9. Lu, P.; Hsieh, Y.-L. J Membr Sci 2010, 348, 21.
10. Mayya, K.; Gittins, D.; Dibaj, A.; Caruso, F. Nano Lett 2001, 1, 727.
11. Gittins, D.; Caruso, F. Adv Mater 2000, 12, 1947.
12. Li, B.; Shen, L.; Liu, X.; Zhang, S.; Wu, C.; Liu, W. Mater Sci Eng A 2004, 364, 324.
13. Caruso, F.; Caruso, R.; Mohwald, H. Science 1998, 282, 1111.
14. Crouzier, T.; Boudou, T.; Picart, C. Curr Opin Colloids Interf Sci 2010, 10, 417.
15. Boddohi, S.; Almodóvar, J.; Zhang, H.; Johnson, P. A.; Kipper, M. J. Colloids Surf B Biointerf 2010, 77, 60.
16. Guyomard, A.; Muller, G.; Glinel, K. Macromolecules 2005, 38, 5737.
17. Picart, C.; Lavalle, P.; Hubert, P.; Cuisinier, F. J. G.; Decher, G.; Schaaf, P.; Voegel, J.-C. Langmuir 2001, 17, 7414.
18. Díez-Pascual, M.; Wong, J. E. J Colloid Interf Sci 2010, 347, 79.
19. Liu, H.; Hsieh, Y.-L. J Polym Sci B 2002, 40, 2119.
20. Lu, H.; Hu, N. J Phys Chem B 2006, 110, 23710.
21. dos Santos, D. S., Jr.; Bassi, A.; Rodrigues, J. J., Jr.; Misoguti, L.; Oliveira, O. N., Jr.; Mendonça, C. R. Biomacromolecules 2003, 4, 1502.
22. Yu, D.; Jou, C.; Lin, W.; Yang, M. Colloids Surf B Biointerf 2007, 54, 222.
23. Mitsuya, H.; Looney, D. J.; Kuno, S.; Ueno, R.; Wong-Staal, F.; Broder, S. Science 1998, 240, 646.
24. Ruan, Q.; Zhu, Y.; Li, F.; Xiao, J.; Zeng, Y.; Xu, F. J Colloid Interf Sci 2009, 333, 725.
25. Du, J.; Hsieh, Y.-L. Cellulose 2007, 14, 543.
26. Hsieh, Y.-L. Text Res J 1995, 65, 299.
27. Cakic, M.; Niholic, G.; Ilic, L.; Stankovic, S. Chem Ind Chem Eng Q 2005, 11, 74.